R. Vanselow R. F. Howe (Eds.)

Chemistry and Physics of Solid Surfaces VII

With 315 Figures

ISBN 3-540-50044-8
0-387-50044-8

Springer-Verlag Berlin Heidelberg New York
London Paris Tokyo

1988

11. Critical Phenomena of Chemisorbed Atoms and Reconstruction — Revisited

Theodore L. Einstein

Department of Physics and Astronomy, University of Maryland
College Park, MD 20742, USA

In the theory of critical phenomena of lattice models, two dimensions holds special fascination for several reasons. In this low dimensionality, fluctuations are stonger, leading to more pronounced divergences near the transition and to grosser violations of mean field predictions. In contrast to three dimensions, there are several exactly-solved models, which provide invaluable benchmarks for understanding critical properties. One of the few places one can hope to find realizations of such models is at surfaces of materials, either by adsorbed atoms or by reconstruction [11.1] of the top layer(s). Regarding reconstruction, 2D does not mean planar: In many reconstructions, several layers near the surface are involved. All that is required for the transitions to be 2D is that displacements eventually decay exponentially as one goes deep into the bulk and that there be no new periodicity exhibited by the ordered state perpendicular to the surface, just parallel to it. On the other hand, we will not consider "ordinary" surface transitions, i.e., 2D critical behavior at the surface generated by a bulk, 3D transition [11.2].

In volume IV of this series [11.3] I reviewed such critical behavior for chemisorbed atoms. At that time, we at Maryland had just reported [11.4] exponents for p(2x2) O/Ni(111) which differed from those expected: Ising-like rather than 4-state Potts-like. When several explanations proved unsatisfying [11.3,5], we undertook a series of painstaking simulations of generic lattices with sizes comparable to those of defect-free regions on typical metal surfaces (~4000 sites). This finite size limits how close one can approach the transition; a key question, requiring explicit calculations, is whether one can in fact get close enough to gauge critical behavior. A goal was to anticipate with ideal data what good experiments would show. In the course of this work we learned many things useful for doing future experiments. These ideas have been published in four rather lengthy papers [11.6-9]. I am grateful to the editors for the second opportunity to present these findings in a unified and hopefully accessible format.

This chapter will begin with a brief review of important concepts. Ideally, the interested reader will look at the earlier review [11.3] or a general reference [11.10] since time forbids a complete recap here.

(Moreover, it may be interesting to find what we did not understand then!) Realistically, few will; thus, the following is intended to be self-contained. In Sect.11.2, I go through many of the findings from our analyses of simulations, stressing ideas that might guide experiments. Topics are highlighted at the start of most paragraphs to permit quick access to topics of special interest and to facilitate skimming. In Sect.11.3, I describe experimental progress since 1981. This section is lamentably shorter than I would have predicted in 1981, and also shorter than the detailed account of what might be expected, presented in the preceding section . Since the discussion is couched in terms of these expectations, readers who plowed through Sect.11.2 will be rewarded and those who did not, can look back. Section 11.4 presents my views on where the field is headed.

This review focuses on chemisorption and reconstruction, since reviews here in 1983 [11.11] and especially 1985 [11.12] emphasized the physisorption cases and since our lattice gas calculations seem more generally applicable. For a somewhat broader review, albeit for a very different audience, see [11.13]. Another somewhat more general and comprehensive review was recently written by *Unertl* [11.14].

11.1 Brief Recap

We specialize here on phase transitions of lattice gas models, typically studied by varying temperature T at fixed coverage. It is usually more convenient to use a reduced temperature $t \equiv (T-T_c)/T_c$. The ordered state at low T (t<0) leads to new sets of spots in a diffraction experiment at positons we shall denote $\{\mathbf{k}_0\}$. If the lattice gas has N sites, the intensity of these new spots, as $t \rightarrow 0^-$, has the form (for N large)

$$I(\mathbf{k}_0,T) \propto N^2(-t)^{2\beta} \ . \tag{11.1}$$

Here β is the exponent associated with long-range order, typically called the magnetization exponent based on the analogy with magnetic systems. Near T_c, there will be strong fluctuations, leading to additional, critical scattering with intensity.

$$I(\mathbf{k}_0,T) = N\chi_{\pm} \left|t\right|^{-\gamma} \text{ for } t \gtrless 0 \ , \tag{11.2}$$

in analogy with the spin susceptibility, χ, in magnetic systems. The *inverse* width of the critical scattering is associated with the correlation length of these fluctuations:

$$\xi(T) = \xi_{\pm} \left|t\right|^{-\nu} \text{ for } t \gtrless 0 \ . \tag{11.3}$$

In addition, energy fluctuations lead to a divergence of the specific heat, having the form

$$C(T) = N\, C_{\pm} \left|t\right|^{-\alpha} + \text{const.} \tag{11.4}$$

For physisorption systems, particularly with grafoil substrates (so that there are many layers of adsorbate), this property can be measured directly sensitively; for chemisorption systems, such measurements are not feasible since the substrate contribution masks that of the surface. Contrary to a statement in [11.3], however, the specific heat can be measured for chemisorption or reconstruction systems, using a scattering experiment, by low-resolution monitoring of the energy-like anomaly in correlation functions [11.7], to be described below (Sect.11.3.3).

In principle, one should allow for different exponents α', γ', ν' below T_c. As a consequence of the scaling hypothesis (which says that ξ is the only important length in the critical regime), these primed exponents are expected to be the same as their unprimed counterparts. Hyperscaling further interrelates the exponents, so that only two are predicted to be independent. In 2D, these have the simple form

$$\alpha = 2 - 2\nu \quad \text{and} \quad \gamma = 2(\nu - \beta) \ . \tag{11.5}$$

The fascination of the exponents is that they are "universal", determined only by the spatial dimension (here 2) and the symmetry of the ordered state relative to the higher-T disordered state. They do *not* depend on any of the microscopic interactions of the system, which in contrast do determine T_c. In addition, the "critical amplitude ratios", C_+/C_-, χ_+/χ_-, and ξ_+/ξ_-, are universal quantities, although the individual amplitudes themselves are non-universal. Moreover, the correlation length ξ is not uniquely specified - nor, for that matter, is the order parameter and its fluctuations χ - and the critical amplitude ratio depends on which definition is used.

To predict the universality class of the disordering of a particular ordered state, one compares the expansion of the Landau-Ginsburg-Wilson Hamiltonian to that of well-studied magnetic systems [11.3,15]. In this framework, continuous transitions of adsorbed atoms are predicted to occur in just four distinct classes (see Table 11.1). Three can be described by q-state Potts models [11.16], with q = 2, 3, 4. These models can be described by the Hamiltonian

$$H = -J \sum_{\langle i,j \rangle} \delta_{S_i,S_j} \tag{11.6}$$

where the subscript denotes lattice sites, and the sum is over nearest neighbors. In essence, in this model each site can have one of q colors, called S_i from analogy to a spin (pointing to the q vertices of a regular polyhedron in a q-1 dimensional spin space). If neighboring sites are the same color, there is an (attractive) interaction. Otherwise, there is

Table 11.1. 2D Universality Classes, Exponents, and Examples

Universality Class	α	β	γ	ν	Sample pattern (full list in [11.3,15] + Example)
Ising (2-state Potts)	0(log)	1/8	7/4	1	c(2x2)/square, rectangular Cl/Ag(100)
X-Y with cubic anisotropy	non-universal!				(2x1)/centered rectangular: O/W(110) (2x1)/square: W(100)
3-state Potts	1/3	1/9	13/9	5/6	($\sqrt{3}$x$\sqrt{3}$)/triangular noble gas/graphite
4-state Potts	2/3	1/12	7/6	2/3	p(2x2)/triangular O/Ru(0001) [graphitic] (2x2)/honeycomb H/Ni(111)?
1st order	1	0	1	1/2	p(2x2)/honeycomb
chiral 3-st. Potts	1/3	1/9	13/9	5/6	(3x1)/centered rectangular

either no interaction or (with slight modification of H [11.16]) a repulsion (such that with random "coloration" the interaction is zero). The origin of the correspondence between the Potts and the lattice gas models does not arise from any microscopic mapping of one Hamiltonian into another. Instead, it has to do with the interaction between fluctuating ordered domains. Thus, for example, the ($\sqrt{3}$x$\sqrt{3}$) R 30° on a triangular lattice, which has three degenerate ground states (say A, B, C), is in the 3-state Potts universality class. Casual inspection [Ref.11.3, Fig.4] shows that the boundary between like domains will have one energy while the boundary between any pair of unlike domains will have a different energy; of course, it is the free energy rather than just the energy that matters. (Furthermore, closer inspection shows that there is a triaxial chirality involved, in that A-B, B-C, and C-A boundaries are different from B-A, C-B, and A-C. But this difference turns out not to change critical behavior [11.17,18]; it is "irrelevant" in a renormalization group sense.) The 2-state Potts model is just the familiar Ising model. This model applies to systems in which there are just two degenerate ordered states, i.e., each atom faces an "either-or" choice in some sense.

According to conventional Landau theory, the overlayer-induced spots must occur at high-symmetry positions of the surface Brillouin

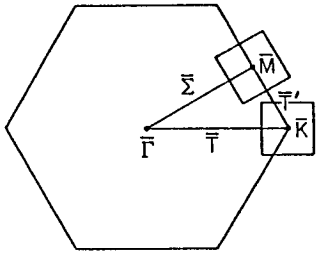

Fig.11.1 Surface Brillouin zone for a triangular substrate. Ordering with ($\sqrt{3}$x$\sqrt{3}$) R30° and p(2x2) symmetry correspond to peaks at $\bar{K}$ and $\bar{M}$, respectively. These two positions for $\mathbf{k}_0$ are the only ones at which, according to conventional Landau theory, continuous disordering can occur. The structure factor was computed along the high-sysmmetry lines and within the appropriate squares (adapted from [11.6])

zone (SBZ) in order for the transition to be continuous: $\mathbf{k}_0$ in this case is at a corner and in other cases may be at a midpoint of an edge (Fig.11.1). Thus, e.g., the (7x7) reconstruction of Si(111) [11.19], c(4x2) CO/Ni(111) [11.20], and the c(2x8) reconstruction of Ge(111) [11.21] are expected to disorder discontinuously (first-order) if they do not go to an incommensurate ordered state (which apparently occurs for Ge [11.21]). As usual in 2D, one must be wary of mean-field like arguments. (E.g., it is well-known that conventional Landau analysis predicts incorrectly that 3- and 4-state Potts models do not disorder continuously because their expansions have cubic terms [11.15]). Below, we will consider the (3x1) on a centered rectangular lattice, which obviously violates this high-symmetry criterion but disorders continuously to an incommensurate disordered state (as required since $\mathbf{k}_0$ is not a point of high symmetry). Finally, there is the possibility of observing critical-like behavior at a first-order transition. As an example, we have studied the p(2x2) on a honeycomb lattice. (For q > 4, Potts models have first-order transitions; this p(2x2) honeycomb has 8 degenerate ordered states.) For further details on Landau classification, see [11.3, 15].

Corrections to the pure power-law behavior of (11.1-4) become evident as one gets farther from T_c. Specifically, one speaks of corrections to scaling of the form

$$|t|^{-\lambda}\left[1 + D_{1,\pm}|t|^{\Delta_1} + D_{2,\pm}|t|^{\Delta_2} + \ldots\right]. \qquad (11.7)$$

At least, there will be analytic corrections ($\Delta_1 = 1$, $\Delta_2 = 2$,...), due e.g., to ambiguities in defining t, as in the special case of the Ising model [11.22]. (If the definition of t happens to correspond to a "pure field", the leading correction may be of even higher order, e.g., $\Delta_1 = 2$ for the Ising model [11.23]). More often, there are weaker ("confluent") singularities, i.e., $\Delta_1 < 1$. These exponents are universal, but the amplitudes, the D's, are not, and some may vanish. In special cases, the leading correction can be logarithmic, eventually dwarfing "pure" behavior close enough to T_c. We have argued [11.24] that the effect of multiple scattering - sometimes claimed to obscure critical behavior in

LEED [11.25] - is simply to alter (not necessarily increase) the size of the D's. (For light adatoms, the atomic scattering function has a pronounced minimum at ~90° [11.26], so with normal incidence one can minimize scattering within the overlayer [11.4]. Hence, by varying the incident angle, one can check for such effects.)

The critical exponents described above are defined in terms of fixed field (here chemical potential) rather than fixed coverage, typically used in chemisorption experiments. If this "isochore" passes near a maximum in the phase diagram, there is no problem. At coverages away from such "saturation" values, one encounters Fisher renormalization [11.27], by which $\beta \rightarrow \beta/(1-\alpha)$ and similarly for γ and ν, while $\alpha \rightarrow -\alpha/(1-\alpha)$, see (11.15 and 16). Thus, the transition is smoothed.

In light of the importance attached to ξ as the only important length in the critical region, it is fruitful to catalog all significant lengths in discussing phase transitions. The characteristic size of defect-free regions of the substrate, L_s, limits the growth of ξ. Once ξ becomes comparable to L_s, we expect the power-law divergences to break down. Correspondingly, this criterion sets a lower limit $|t_{min}| \sim L_s^{-1/\nu}$ of closest approach to T_c; for smaller t, the data is contaminated by finite-size effects. With the notable exception of graphite, most substrates studied to date have L_s on the order of 100's of Å. Another length due to the instrument used for measurements is the characteristic distance L_i over which correlations are sampled coherently. In LEED, L_i is typically the transfer width of the instrument response function [11.28]. For conventional LEED systems $L_i \gtrsim 100$ Å, but high-resolution systems can achieve L_i's nearly an order of magnitude larger [11.29]. Atom scattering (Chap.14 and [11.30]) can also attain L_i's up to ~500 Å, but electrons tend to be easier to use. In the critical region, when $\xi << L_i$, one has the diffraction limit, while in the opposite limit one probes short-range order and finds energy-like anomalies. The corrections to scaling, which enter away from T_c when ξ is small, may be associated with small length scales such as the lattice spacing or the electron inelastic mean-free path (if one is considering multiple scattering).

More strikingly, there may be weak but relevant fields which lower the symmetry of the Hamiltonian. Close to T_c one then observes scaling associated with the lower symmetry system, but when ξ decreases to a size comparable to the characteristic length associated with the field, there is crossover to scaling appropriate to the higher-symmetry system. Such behavior was indeed invoked [11.31] to try to explain our O/Ni{111} exponents. The form of the crossover function is generally unknown, but in some cases the general form has been computed using renormalization group methods [11.32].

11.2 Results from Computed Structure Factors

11.2.1 General Features

As described in the introduction, we used Monte Carlo methods to produce ideal "data" for generic lattice gases [11.6-9]. Since much exact work existed already for Ising models, we considered models which had $(\sqrt{3}x\sqrt{3})$ R 30° and p(2x2) ordered structures on triangular lattices [11.6,7]. We used a lattice with 3,888 sites (comparable to the size of defect-free regions on good metal surfaces) a hexagonal perimenter, and periodic boundary conditions. We fixed the chemical potential such that the coverage near T_c was close to saturation. For the $\sqrt{3}x\sqrt{3}$ overlayer, the Hamiltonian was the simplest possible:

$$H = E_1 \sum_{\langle ij \rangle_1} n(\mathbf{r}_i)\, n(\mathbf{r}_j) \tag{11.8}$$

where $n(\mathbf{r}_i) = 0, 1$ is the occupancy of the lattice site at $\mathbf{r}_i$ and the nearest neighbor repulsion E_1 was fixed at 1 to set the energy scale. For the p(2x2), a second neighbor repulsion E_2 is also needed; it was set to $E_1/2$. Further details are given in [11.6].

We computed the structure factor

$$S(\mathbf{k},T) = \left\langle \left| \sum_j n(\mathbf{r}_j) \exp[i(\mathbf{k}+\mathbf{k}_0)\cdot\mathbf{r}_j] \right|^2 \right\rangle \tag{11.9}$$

which is just proportional to the intensity one would measure in the kinematic limit. A series of contour plots in [11.6] nicely illustrates the narrowing and increase in intensity of $S(\mathbf{k})$ as one approaches a continuous phase transition. The novice is encouraged to look at the two pages of plots (Figs.2 and 3 of [11.6]). The best way to analyze the wealth of data - not yet applied to any adsorption experiment - is to take cognizance of the phenomenologically predicted scaling form [11.10]

$$S(\mathbf{k},T) = a_1 |t|^{-\gamma} X_{\pm}\left[a_2 |t|^{-\nu} |\mathbf{k}| \right] \tag{11.10}$$

for small $|t|$ and $|\mathbf{k}|$; $X_{\pm}(y)$ are universal functions of $y = k\xi$, while a_1 and a_2 are system-dependent constants. Figure 11.2 shows such a plot for the $\sqrt{3}x\sqrt{3}$ system with $\mathbf{k}$ running from the corner of the SBZ ($\bar{K}$ of Fig.11.1) toward the center ($\bar{\Gamma}$) using 3-state Potts values of γ and ν and with T_c picked to give the best scaling. To within statistical error, $\mathbf{k}$'s up to half way to the center can be made to scale. Multiple scatter-

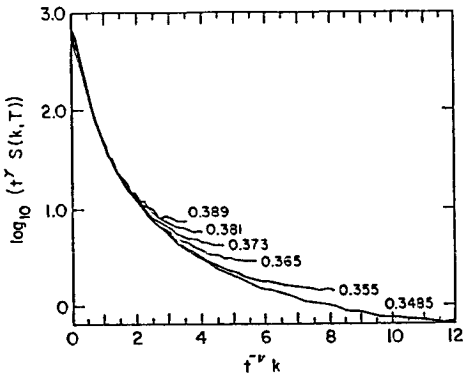

Fig.11.2 Structure factor above T_c scaled according to (11.10) for the $\sqrt{3}x\sqrt{3}$ case, assuming γ and ν of the 3-state Potts model and $T_c/E_1 = 0.338$, with **k** along $\bar{T}$, starting from $\bar{K}$ (from [11.6])

ing could decrease (or increase) this cut-off. Once the correlation length becomes comparable to the size of the system L_s, the universal behavior of (11.10) as well as (11.1-4) break down due to finite-size effects. Here, data within about 2% of T_c cannot be made to scale. Recall that since the amplitude of ξ is not universal, t_{min} will be the value of t, for a given size lattice, below which finite-size breakdown sets in.

11.2.2 Diffraction-Limit Results

Finding T_c: The more conventional analysis involves separating $S(\mathbf{k},T)$ into various measurables and using log-log plots (vs t) to estimate exponents. Adopting as the criterion for T_c that value which maximizes the linearity of the log-log plot over some thermal range, careful analysis in [11.6] shows that the convergence of T_c is faster than that of the effective exponents, so that the lack of knowledge of T_c does not unduly affect the ability to estimate exponents. In Sect.11.2.3, we will discuss an alternate way to estimate T_c using a point of inflection. In this experiment one finds scaling over less than two decades of reduced temperature, usually only about one, so that it is hard to get a sense of convergence.

Finding χ, ξ: We first consider the diffraction limit [11.10] $k\xi << 1$ or $\xi << L_i$. In this limit, S separates into a contribution from long-range order below T_c and critical scattering peaking at T_c. In the following, $\chi(T)$ and $\xi(T)$ are determined as those values which, at each T, minimize a least-squares fit of $\{S(\mathbf{k},T)\}$ to a Lorentzian form, $\chi/(1 + \xi^2|\mathbf{k}|^2)$. Near T_c, the fit is insensitive to the large-k cutoff. (Since this definition ignores possibly sizable non-Lorentzian behavior near T_c, the χ and ξ differ somewhat from conventional definitions but nonetheless have the same critical properties.) Below T_c one must also

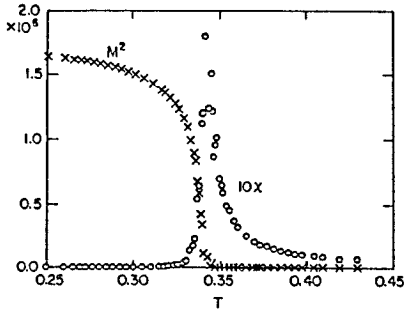

Fig.11.3 Temperature dependence of χ and of M^2 for the $\sqrt{3}x\sqrt{3}$ case. Note the large critical amplitude ratio of χ above and beneath T_c; experimentally deducing exponents for critical scattering below T_c is difficult if not impossible. Note also the different dependence on the number of scatterers N, indicated in eqs.(11.1,2) (from [11.6])

worry about the δ-function contribution from long-range order, called M^2 in Fig.11.3 based again on the analogy with magnetic systems. With our periodic boundary conditions, this contribution only occurs at $\mathbf{k}_0$, i.e., $\mathbf{k} = 0$, but in an experiment (or simulation with other boundary conditions) this term would be spread over a width proportional to the inverse size, i.e., $N^{-1/2}$; this neighborhood of $\mathbf{k}_0$ would have to be excluded from the least-squares fitting. Once T_c is estimated, (above T_c) one can include data at $\mathbf{k} = 0$ (or $\mathbf{k} \simeq 0$ in an experiment) to decrease noise. While one can imagine other schemes to extract χ and ξ, one must be careful not to weight large-k data excessively. For example, if one takes ξ^2 from the least-squares fit of $S^{-1}(k)$ vs k^2, $k\xi$ is not small, and the "wrong" critical behavior is observed [11.6].

Thermal cutoffs: The divergence of ξ will be limited by the size of defect-free regions, and when ξ becomes comparable to this size, scaling breaks down. Since in these experiments (or simulations) one has little data to spare, one should not remove a larger range around T_c than necessary. The procedure suggested in [11.3] - analyzing all the data that appear to scale - is dangerous in that one might choose T_c so that data near it scale when they really should not. One is particularly prone to this poor choice when the thermal range of data is small. An objective criterion is to exclude data which are more than some specific fraction of the maximum correlation length found. In our case, we used the fraction 1/2, but with non-periodic boundary conditions, the maximum ξ will be smaller, and this criterion might cause one to discard more data than necessary. Since this procedure involves non-universal features, it is not possible to give strict prescriptions. At the other limit, far from T_c, ξ decreases to the size of other lengths in the problem (e.g. the lattice spacing) and corrections to scaling become large. Again, the experimenter must exercise judgement. In our case, we could sometimes use data as far as 25% away from T_c in log-log plots.

Definition of t: Above T_c, we redefined [11.33] the reduced temperature t as $1 - (T_c/T)$. In some cases [11.33] this definition has led

to smaller corrections to scaling - the two definitions differ by a term of order t^2. The difference in the exponents from the two definitions is on the order of the statistical errors. Some experts prefer this alternative defintion since it corresponds more closely to the form appearing in renormalization group calculations [11.34].

Results and statistical errors, $T < T_c$: In Table 11.2 are listed under "effective" the results of the log-log fits for $0.003 < t < 0.25$; the pure exponents are taken from Table 11.1. While T_c is non-universal, it was corroborated using several other more sophisticated numerical techniques. The level of accuracy is seen to be of order 10%, good enough to distinguish between universality classes but not much more. The error bars, of order 10% again, were based on standard error propagation techniques starting from 2-5% errors in the $S(\mathbf{k},T)$. Similar errors are to be expected from good experiments. Given the linearity of the fits (Fig.11.4), the estimate of the exponents did not change beyond the error bars when either upper or lower thermal cutoff was varied. The estimates are quite sensitive to the estimate of T_c: a 12% variation in the estimated T_c produced a 17% variation in the deduced γ.

Problems for $T < T_c$: Below T_c the contribution due to long-range order, called M^2, can be extracted from $S(\mathbf{k},T)$ by subtracting

Table 11.2. Summary of Computed Exponents

	√3x√3			p(2x2)	
	Pure	Effective		Pure	Effective
kT_c/E_1	-	0.338±0.002		-	0.344±0.002
γ	1.44	1.25±0.07		1.17	1.13±0.06
ν	0.83	0.77±0.05		0.67	0.70±0.09
β (Δ=1)	0.111	0.104±0.010	(Δ=1)	0.083	0.083±0.009
(Δ=1)(min χ^2: T_c = 0.335)		0.087±0.010	(Δ=1) T_c = 0.343		0.078
no Δ, max linearity T_c = 0.334		0.078±0.010	no Δ T_c = 0.343		0.065
Δ=2/3 T_c = 0.336		0.111±0.019	$(\log\|t\|)^{1/8}$ T_c = 0.343		0.077±0.020

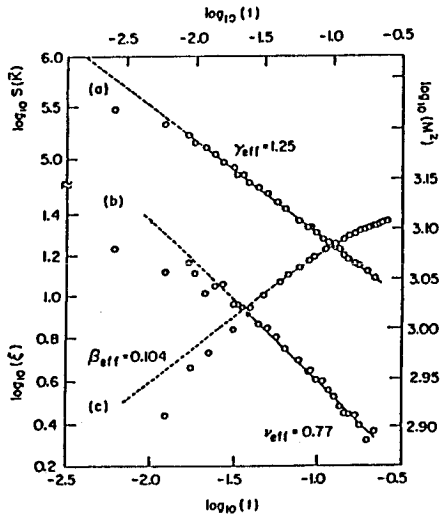

Fig.11.4 Log-log plots for the $\sqrt{3}x\sqrt{3}$ case. a) χ above T_c, b) ξ above T_c of M^2 below T_c. The thermal scale at the top applies to c), that at the bottom to a) and b). The fit in c) includes a nonlinear term in the fitting function (from Ref.11.13, adapted from [11.6])

$\lim_{k\to 0} S(\mathbf{k},T)$, based on some fit (Fig.11.3). For large system size - larger than here - (11.1 and 2) suggest this subtraction is unnecessary, since the critical scattering is of order 1/N compared to M^2. Far from T_c, χ is small and need not be removed. In a plot of log M^2 vs log $|t|$, depicted in Fig.11.4, nonlinearities are clearly present; no choice of T_c will remove them. Evidently, corrections to scaling are larger below T_c than above. Since ratios of corresponding amplitudes of these corrections above and below T_c [e.g., D_{1+}/D_{1-} in (11.7)] are universal, we expect this behavior to be general. If larger defect-free regions were achievable, one could simply use data closer to T_c and discard more data at large $|t|$. Since this is not the case, one must cope with the corrections. Without additional information, the simplest approach is to assume analytic corrections (Δ_1=1) and so fit M^2 to $(|t|+Dt^2)^{2\beta}$, but with T_c at the value determined above the transition. The results are listed in Table 11.2. For the $\sqrt{3}x\sqrt{3}$ the β_{eff} is 6% too low, but within error bars, while for the p(2x2) there is fortuitous agreement. If, instead, T_c is freed and fit along with the slope, then in both cases the estimate of T_c declines (by 1% and 1/3%, respectively) and the estimate of β drops considerably (by 16% and 6%, respectively). Thus, in fitting exponents below T_c, without knowledge of T_c, one does better by using the estimate of T_c found from critical scattering *above* T_c. Lyle Roelofs had realized this already while analyzing data for O/Ni{111} [11.4], but we thought it was due to limited data below T_c. For the two models under study, Δ_1 is known in advance from theoretical work. For the 3-state Potts model, $\Delta_1 = 2/3$ [11.35]; with this ansatz, we estimate $\beta = 0.111 \pm 0.019$ (fortuitous exact agreement) and

$T_c = 0.336 \pm 0.002$. For the 4-state Potts model, the leading correction is logarithmic [11.16,36], a general feature of classes of models at the last value of some parameter at which the transition is continuous. (For $q > 4$, Potts models have first-order transitions.) As seen in Table 11.2, fitting [11.36] to $|t|^{2\beta}\cdot(1+D[\ell n|t|]^{1/8})$ does not improve agreement of β with the pure value. For the Ising model, remarkably, there are no low-order non-analytic corrections to scaling [11.22]. Note that the amplitudes of the corrections to scaling are non-universal, and may even vanish. This happens, for instance, in the Baxter-Wu model, a member of the 4-state Potts class [11.16]. Finally, we tabulate the effective β when no corrections are included for our two systems; in both cases, the exponent is much too low.

Critical scattering below T_c unobservable: In our model systems, we can similarly compute the exponents γ' and ν' associated with critical scattering in the ordered regime. The former in particular shows strong nonlinearities in log-log plots. However, the amplitude of this critical scattering is quite small. We computed the critical amplitude ratio χ_+/χ_- as about 40 for both these models and for their Potts analogues. (For the Ising model, it is known to be nearly 38 [11.37]). For the correlation length, the corresponding ratio is about 4 [11.37] (somewhat lower for the $\sqrt{3}x\sqrt{3}$). Intuitively, one is tempted to use these ratios to interpret the more rapid onset of corrections to scaling below T_c: the (diverging) correlation length and susceptibility which manifest the critical region decrease much more rapidly below T_c than above as $|t|$ increases.

Asymmetries: Lattice symmetry (Fig.11.1) dictates that the contours of $S(\mathbf{k},t)$ have only 3-fold and 2-fold symmetry, respectively, in our two systems, much lower than the analogous Potts systems. In a small $|t|$ expansion of $S(\mathbf{k},t)$ (around $\mathbf{k}_0$), one can write

$$S(\mathbf{k},T) = \chi(T)\Big(\big[\,1 - \xi(T)^2\,|k|^2\big] + b(T)f(k_r,k_a) + \ldots\Big)\,, \qquad (11.11)$$

where k_r, k_a are the radial and azimuthal components of k (with respect to the center of the SBZ); $f = k_r^3 - 3k_a^2\,k_r$ for the $\sqrt{3}x\sqrt{3}$ and $f = k_a^2 - k_r^2$ for the p(2x2). These definitions of χ and ξ differ slightly from those used earlier, but have the same critical properties. Analysis of b(T), as explored in [11.6], gives interesting insights into the asymmetries in domain wall energies which complicate these lattice gases compared to their Potts analogues. With present system sizes and resolution, we do not believe these features can be well measured, but this prospect does offer a keen challenge to the experimentalist.

11.2.3 Energy-Like Limit

In the other limit, $k\xi >> 1$, $X_\pm(y)$ of (11.10) also has a simple expansion [11.10] known to experts in critical phenomena for nearly two decades [11.38] but not applied to surface problems until recently:

$$X_\pm(y) = C_1 y^{-\gamma/\nu}\,[1 + C_2^\pm\, y^{-(1-\alpha)/\nu} \pm C_3\, y^{-1/\nu} \ldots]\,. \qquad (11.12)$$

The leading term cancels the susceptibility prefactor of (11.10); the first and third terms are analytic, while the second has an energy-like anomaly. (Its first derivative is like a specific heat, while its integral is the [singular part of the] free energy.) Note that for an infinte system with $k \neq 0$, $k\xi >> 1$ can always be achieved if one gets close enough to T_c; for $k \neq 0$, $S(\mathbf{k},T_c)$ must have an energy-like anomaly. This behavior is intimately related to the observation that two-site or multisite correlation functions, i.e., $\langle n(r)n(r+R)\rangle$ or $\langle n\ n\ n\rangle$, etc., as functions of T, have energy-like anomalies near T_c: $\mathcal{G}_1 \mp \mathcal{G}_2|t|^{1-\alpha}$; more precisely, it is combinations of such correlation functions that are insensitive to the phase of the order-parameter, such as $\Sigma_r\langle n(r)n(r+R)\rangle$. Recalling the lattice gas Hamiltonian (11.8), we see that these correlation functions are, up to multiplicative constants, the constituents of the energy; this is the basis of the expansion in (11.12). (See [11.7,39] for a more formal derivation). While this discussion suggests that α might be measured in photoemission, core shifts, etc. [11.40], in general, the shifts seem to be too small and the precision inadequate.

LEED integrated intensity: If one measures the integrated intensity in LEED, these effects should be evident:

$$I(k_I,T) = \int_0^{k_I} dk\ k \int d\theta_k\ S(k,T)$$

$$\sim A_0 \mp B_\pm\,|t|^{1-\alpha} - A_1 t \ldots\ [T \gtrless T_c] \qquad (11.13)$$

The three coefficients depend on k_I; the A's come from the analytic part. The right side is valid only when k_I is "large enough", i.e., close to T_c and for moderately large integration radius. Again, the thresholds are non-universal, so our numerical studies give suggestive rather then definitive values. Once ξ grows comparable to the size of the defect-free regions, there will again be finite-size rounding; in this case that means that $I(k_I,T)$ will be analytic over a small neighborhood near T_c, which should be removed from fits. This behavior is illustrated in Fig.11.5. (The range of t over which this smearing occurs need not be the same as in the diffraction limit, since a different definition of ξ may be involved, with a different $\xi_\pm$.) At the other limit of the scaling range, there is no evidence that corrections to scaling

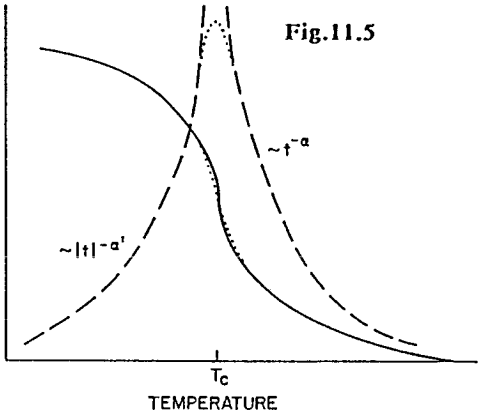

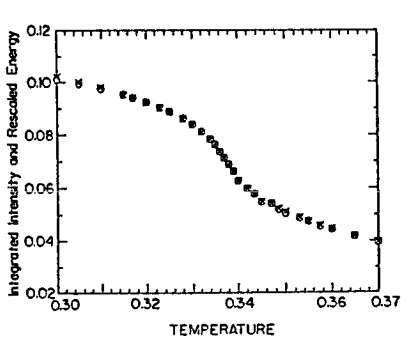

Fig.11.5 Schematic of the energy-like anomaly associated with positive α, as given in (11.13), seen by monitoring the integrated intensity around an overlayer-induced, extra spot in a diffraction experiment (solid line). The derivative with respect to temperature (dashed line) diverges like the specific heat, illustrating that the point of inflection of the solid curve offers a good estimate of T_c. The dotted lines indicate the finite-size rounding which occurs in real systems when the correlation length ξ exceeds the size of the defect-free regions L_s. Far away from T_c, when $\xi << L_i$, the solid curve is given by (11.1) [(11.2)] below [above] T_c, plus presumably large corrections to scaling (from [11.41])

Fig.11.6 Illustration of eq. (11.14): Structure factor integrated over 2.3% of the surface Brillouin zone [circles] vs. T, plotted with the rescaled energy [x's] for the $\sqrt{3}x\sqrt{3}$ case. The energy like behavior of the integrated structure factor near T_c is evident (from [11.7])

enter more quickly below T_c, although we have not considered this problem carefully.

Illustration of energy-like behavior: The key point to verify is that for adequate k_I, the intensity behaves like the energy:

$$I(k_I,T) = -u(k_I)\, E(T) + w(k_I) \qquad (11.14)$$

As k_I is increased, the largest $|t|$ at which (11.13) holds increases, but the size of $B_\pm/A_0$ decreases. Figure 11.6 coplots the left and right sides of (11.13) for $k_I \sim 5/36$ of the distance from the corner of the SBZ (k_0), to the SBZ center, i.e., 2.3% of the SBZ area. (The parameters u and w were determined by a least-squares fit.) For this temperature range and k_I, $I(k_I,T)$ gives the same information about the critical behavior as the [internal] energy, or for that matter, its directly measurable derivative, the specific heat. (This correspondence continues to hold over the finite-size-rounded region.) An important corollary is that *the point of inflection of $I(k_I,T)$ corresponds to the peak of the specific heat* [11.7,41]; this fact justifies the common LEED practice [11.42] of using the point of inflection as a "best estimate" of T_c. For the simple Ising model, we have, in fact, determined the A_i, $B_\pm$ exactly [11.7].

As a further test, we determined the effective α using the right side of (11.13) to fit $I(k_I,T)$ as well as the energy. For Potts models with continuous transitions, duality arguments show $B_+ = B_-$ [11.45] (and scaling dictates $\alpha' = \alpha$), reducing the number of fitting parameters. We also tried fits with $A_1 = 0$ (no linear term). Within statistical errors, similar values were found for fits of E and of $I(k_I,T)$ once the area was 2.3% of the SBZ and certainly once it was 4.6%. To gauge the finite-size-rounded region, we decreased the lower thermal cut-off until the effective α changed significantly; this change occurred below $|t| \sim 0.02$. The effective α decreased considerably when A_1 was included, giving better agreement with the pure value for the $\sqrt{3}x\sqrt{3}$ but poorer agreement for the p(2x2)! To restate the key point, however: if k_I is large enough, the problems encountered in fitting $I(k_I,T)$ are no different from those in fitting the specific heat from, say, a direct calorimetric measurement [11.44,45] (as performed on physisorption but not chemisorption systems) or from direct Monte Carlo calculations [11.46].

To summarize, there are several advantages to this approach. 1) High resolution and cumbersome deconvolution of an instrument response function are not required, so the measurement is comparatively easy. 2) Multiple scattering is intrinsically not a complication. 3) Values of α differ considerably between universality classes (especially in contrast to β). Some caveats are: 1) for Ising systems (α=0 [logarithmic]) or first-order (α=1), the energy anomaly is hard to distinguish from the analytic background. Indeed, for this reason, this method was not used much in 3D, where α is usually small [11.47]. When it is not certain *a priori* whether the disordering is Ising or first-order, this method does not really clarify matters. One way to proceed is to use a coverage well away from saturation. In the Ising case, one expects the logarithmic singularity to become a cusp. If the transition is first-order, one expects a broad smear characteristic of a coexistence region [1.48]. 2) If the thermal fitting range is small and too close to T_c, one might interpret the analytic behavior as evidence of an Ising transition. 3) Given the sensitivity of fits, it is risky to rely on a single exponent to attribute critical behavior to a particular universality class.

11.2.4 Melting to an Incommensurate Disordered Phase

Incommensurate overlayers are characterized by S(k,T) peaking at positions in reciprocal space not simply related to the primitive lattice vectors (i.e., the overlayers' primitive vectors are not simply related to those of the substrate). This behavior says nothing about whether the adatoms are in registry with the substrate as in strong chemisorption, or whether a continuum of adsorption sites are occupied, as in physisorption (Chap.2 and [11.49]) or crystal growth (see, for example

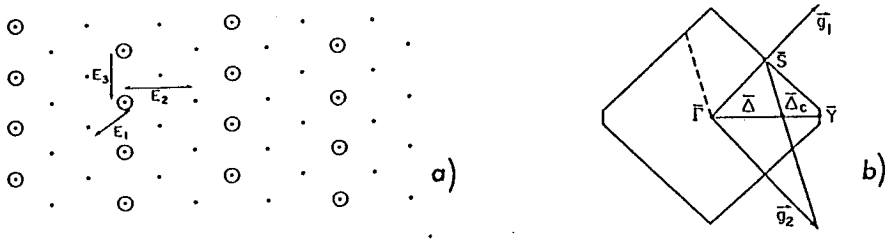

Fig.11.7 a) The (3x1) phase on a centered rectangular lattice, with the interactions producing the ordered overlayer. b) The surface Brillouin zone of this substrate, along with the lines along which the structure factor was computed. Here $\mathbf{k}_0$ is $\bar{\Delta}_c$, a point of low symmetry. From conventional Landau theory, one would (mistakenly) not expect this overlayer to disorder continuously (from [11.6])

[11.50]). On the other hand, it is possible to distinguish between a "floating" phase, in which there are algebraic decay of correlations and so novel behavior of S(**k**,T) [11.51] and a disordered phase, for which decay is still exponential and the analysis of Sect.11.2.2 should apply.

We have studied an example of a transition to the latter by a (3x1) on a centered rectangular lattice. This pattern is illustrated in Fig.11.7a, with the pairwise interactions depicted. In particular, we focus on the case $E_1 = \infty$, $E_2 = 1 = -E_3$, which was explored by *Huse* [11.52] using existing exact results of *Baxter* [11.53]. In the corresponding SBZ, shown in Fig.11.7b, we see that the $\mathbf{k}_0$ associated with order is not a high-symmetry point. (In fact, we had to concoct a Greek letter for it!) Simple considerations of interface energies for the 3 possible ordered domains (A, B, C) shows A|B, B|C, and C|A walls differ from B|A, C|B, and A|C walls. This "uniaxial chirality" is predicted [11.17] to alter the leading critical behavior, in contrast to the "triaxial chirality" [discussed after (11.6)] distinguishing the $\sqrt{3}$x$\sqrt{3}$ from the 3-state Potts model, which merely introduces a correction to the scaling term with a predicted exponent Δ (not to be confused with the SBZ labels!). A basic question is whether the (3x1) can disorder continuously in a single transition. As catalogued in [11.8,54], Landau-like arguments and several continuum studies suggest that a floating phase must intervene, but most numerical studies (including ours) support *Huse* and *Fisher's* [11.17] contention that such a single disordering transition can occur, but (perhaps) in a new universality class.

Scans of S(**k**,T) near the transition are depicted in Fig.11.8. While the long-range-order spike always lies at $\bar{\Delta}_c$, the critical scattering peaks above $\bar{\Delta}_c$ (for our choice of chemical potential), except at T_c. Again, however, the critical scattering satisfies the scaling form of (11.10), but a novel feature is that the peak of $t^{\gamma}S(\mathbf{k},t)$ is not at $k = 0$. (Indeed, the shift of the peak, $q \sim |t|^{\bar{\beta}}$, with the prediction [11.17] $\bar{\beta} = \nu$.) The low symmetry of contours of S(**k**,T) complicates the analysis; the reader is referred to [11.8] for details. One analysis yields γ_{eff} =

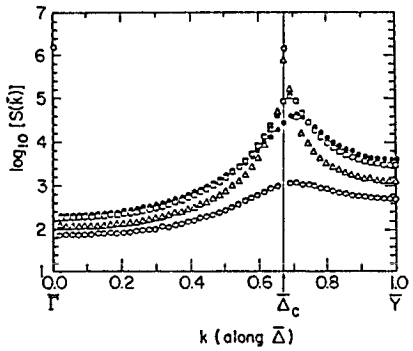

Fig.11.8 Plots of S(k,T) for a 36 x 108 lattice at temperatures about 5% below T_c (circles), at T_c (triangles), 5% above T_c (squares), and 10% above T_c (solid hexagons). Only at T_c does the critical scattering peak at $\bar{\Delta}_c$. For the chosen chemical potential, it peaks above it, for $T \lesssim T_c$. The curves for $T > T_c$ can be scaled as in (11.10), using 3-state Potts exponents (from [11.8])

1.35 ± 0.10 and ν_{eff} = 0.85 ± 0.10, consistent with 3-state Potts values (γ=13/9, ν=5/6). Another analysis gives γ_{eff} = 1.55 ± 0.12, and ν_{eff} = 0.87 ± 0.08 or 0.95 ± 0.09, depending on which direction in k-space is analyzed. Assuming 3-state Potts exponents, the critical amplitude ratios of χ and ξ are 160 ± 80 and 5.0 ± 1.7, much greater than for the $\sqrt{3}$x$\sqrt{3}$ case or for a 3-state Potts model. This behavior is consistent with predictions that the new universality class might have 3-state Potts exponents but a new scaling function. Similarly, in a low-resolution-type procedure following Sect.11.2.3, α_{eff} = 0.45 ± 0.05 (consistent with that analysis without a linear $A_1 t$ term) but B_+/B_- = 3.2 ± 1.3 (rather than unity). If there were an intervening floating phase, then the lower-T transition from the commensurate state should have the Pokrovsky-Talapov form [11.55,56] while the higher-T transition should show Kosterlitz-Thouless [11.55] behavior. In the former, the specific heat diverges as T_c is approached from below but remains finite during approach from above [11.56]. In the latter, the specific heat peaks above the transition in a non-divergent, non-singular way [11.57]. In such a floating-phase scenario, one would not expect that same sort of anomalous behavior above and below the transition. However, in this case one must be unusually wary of finite-size limitations (see [11.8]).

While [11.8] reports several other studies, one is of particular interest: an investigation of $q\xi$ as the transition is approached. In a commensurate phase, this limit should be zero since q "locks in", while in a floating phase it should be ∞ since correlations decay with a power law rather than exponentially. *Huse* and *Fisher* [11.17] predicted this limit to be a universal number, while our studies give a value dependent on chemical potential. Nonetheless, their prediction might be correct, and we - and a potential experimentalist - are just seeing a slow approach to the universal number due to the limited size of our system.

It would certainly be interesting to see an experimental study of such a transition. The system H/Fe{110} was thought to be an example

[11.58] until it was determined - after much misdirected theoretical work [11.59] - that H adsorbs in the quasi-threefold rather than bridge site [11.60]. More generally, incommensurate disordered phases are probably quite common in chemisorption systems, without being so identified. For example, we believe the region labelled "antiphase domains" in our study of O/Ni{111} [11.61,62] is such a case.

11.2.5 Critical Behavior at Temperature-Driven First-Order Transitions

In Table 11.1 there are, perhaps surprising to many, critical exponents for a first-order transition. For example, a leading experimentalist wrote that "critical scattering is an unambiguous hallmark of a second-order phase transition". To the contrary, there are cases in which a first-order phase transition will have all the qualitative features of a second-order one [11.63]. These cases can sometimes arise in the generic situation in which the terminal point of a line of first-order transitions (in, say, a temperature-chemical potential phase diagram) is for some reason not a usual [second-order] critical point. Such first-order transitions are called "temperature-driven" to distinguish them from "field-driven" transitions such as found in crossing the line of first-order transitions, where the more usual first-order discontinuous behavior is found. As a possible lattice gas illustration of this behavior, we have studied the p(2x2) on a honeycomb substrate. With its eight degenerate ground states, this model calls to mind the 8-state Potts model. (However, they are not in the same universality class; e.g., their order parameters have different dimensions.) Recall that for q > 4, q-state Potts models have first-order transitions [11.16], but these transitions are examples of the behavior just discussed. Indeed, Monte Carlo studies of 5- and 6-state Potts models showed disordering behavior barely distinguishable from that of the 4-state Potts model [11.64].

Critical behavior: For the p(2x2)/honeycomb, we proceed as before (see [11.9] for details) to compute S(**k**,T). Since this substrate is not Bravais, there are complications in **k**-space. The 6 integer-order spots $\bar{\Gamma}'$ in the first ring are not equivalent to the specular spot $\bar{\Gamma}$. Also, the outer and inner half-integer, overlayer-induced spots are not connected by a reciprocal lattice vector and so are not equivalent [11.61]. Choosing as $\mathbf{k}_0$ an inner such spot, we perform a log-log analysis and find $\gamma_{eff} = 0.86 \pm 0.20$, $\nu_{eff} = 0.55 \pm 0.15$, and (with a $\Delta = 1$ correction to scaling) $\beta_{eff} = 0.08 \pm 0.03$, compared to the discontinuity fixed-point values of 1, 1/2, and 0, respectively (see, for example, [11.65]). Using γ_{eff} and ν_{eff}, we find that S(**k**,T) satisfies the same scaling form of (11.10) as for the continuous transitions (Fig.11.9). (In a similar plot for the 8-state Potts model, we find best scaling for $\gamma = 0.85$ and $\nu =$

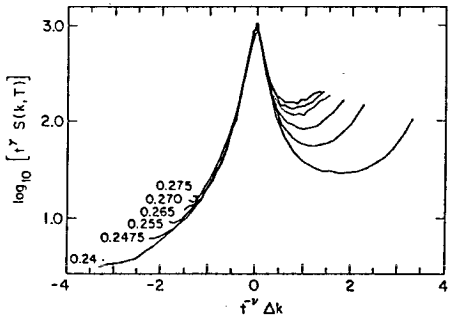

Fig.11.9 Structure γ factor for the p(2x2) on a honeycomb lattice, above T_c, scaled according to (11.10) with $\gamma = 0.86$, $\nu = 0.55$, and $T_c/E_1 = 0.233$. This temperature-driven first-order transition could not be readily distinguished from a continuous transition. The incipient divergences on the right are indicative of a divergent susceptibility at the outer integer-order spots, associated with the (vanishing) binding energy difference between the two Bravais triangular sublattices (from [11.9])

0.6.) The critical amplitude ratios of χ and ξ are much smaller than for the continuous transitions: 13^{-4}_{+11} and 1.1 ± 0.3, respectively.

Much of this work was motivated by attempts to understand our nemesis, p(2x2) O/Ni{111}. As discussed near the end of [11.3], *Schick* suggested an interpretation in terms of a Heisenberg model with corner cubic anisotropy [11.67]. Several aspects of the beam shape, both experimental and in these simulations, seem inconsistent with that explanation [11.9]. Indeed, in other searches of coupling-parameter space we were never able to find the Ising-like behavior of Schick's scenario [11.5].

Inequivalent beams: As noted above, the first ring of integer beams in this model are not equivalent to the specular beam. S(**k**,t) at these outer beams depends not only on the total coverage but also on the difference between the two triangular sublattices of the honeycomb net. This occupation difference is conjugate to a binding energy difference such as one would find between fcc-like and hcp-like sites on a close-packed (fcc or hcp) surface. As explored and depicted in [11.9], there is a susceptibility associated with this field leading to divergent $S(0,T_c)$ at the outer integer spots, even when, as here, the binding energy difference is zero. Unfortunately, it would be difficult to observe such critical fluctuations near an integer beam, but this type of behavior is more general.

In typical diffraction patterns there can be several inequivalent sets of adsorbate-induced spots. One can imagine (though not necessary be able to create in a physical system) a field (i.e., a binding energy difference) which favors one set over others. The susceptibility (or fluctuations) with respect to these fields can be different for each set of spots. If the field turns out to be relevant, then the different spots can have different exponents γ and β [11.10b]. (However, according to

the scaling hypothesis [11.10], there is only one diverging length scale near T_c, so that the ξ's at each spot will have the same ν.) For the p(2x2)/honeycomb, the field associated with the difference between the inner and outer half-order spots is irrelevant, so that the two sets should differ only in amplitudes of corrections to scaling. However, for a p(2x2)/*square* [11.68], the field associated with the difference between (1/2, 1/2) and (1/2, 0) spots is relevant; *Enting* [11.69] predicts the universal relation $\beta_{1/2,1/2} = 4\beta_{1/2,0} - 1/4$. An analogous difference may have been seen for S/W{110} [11.70]. Even more generally, some diffraction features can in principle change discontinuously at a transition while others change continuously (in analogy to transitions where magnetization changes discontinuously while energy changes continuously, or vice versa).

11.2.6 Effects of Defects

In statistical mechanics it is common to make a somewhat arbitrary division of defects into two sorts: annealed and quenched. [11.71,10c] Annealed defects are in thermal equilibrium with the adatoms and, therefore, move around. The simplest case is vacancies, i.e., fixed coverage at a value below saturation. We have already noted that the result is smoothing of the transition, with Fisher renormalization of the exponents. The possibility of vacancies also leads to corrections to scaling, the form of which has been studied for the Ising model [11.23].

In the other limit, the defects are fixed in position [11.72]. In Monte Carlo simulations, this behavior is readily modeled by fixing a number of vacancies (or extra atoms) in random positions and not propagating them. By fixing the occupancy at certain positions, these quenched defects limit the growth of the correlation length ξ, thereby introducing a new length scale of order $N_D^{-1/2}$, where N_D is the defect density. The effect is essentially the same as having a finite-size system in a simulation, or a mean terrace width in an experiment. We have seen that below some $|t|_{min}$, singular behavior is no longer observed. Thus, we expect $|t|_{min} \simeq N_D^{1/2\nu}$ once the defects dominate, a relation we plan to verify numerically and experimentally.

11.3 Experimental Progress Since ISISS-1981

In spite of the many examples of ordered chemisorbed overlayers appearing in catalogues [11.73], the search has been disconcertingly difficult for relatively simple ones to which to apply theoretical concepts of critical phenomena [11.74]. A chemisorption system with a good $\sqrt{3}x\sqrt{3}$ transition has proved particularly elusive; e.g., a recent study of Al/Si(111) found first order behavior [11.75]. (Such transitions are frequently observed in physisorption.) However, a recent careful study [11.45] of the specific heat of H/graphite with a.c. calorimetry shows striking sensitivity to the chemical potential (i.e., to where on the phase boundary the transition occurs).

11.3.1 4-State Potts Systems: O/Ru{0001}

Very recent reports of *Piercy* and *Pfnür's* LEED study of the disordering of p(2x2) O/Ru{0001} [11.76] are, thus, particularly heartening. The integrated intensity of an overlayer-induced spot was measured with a Faraday cup subtending 2.3% of the SBZ. First they determine T_c from the point of inflection as 754 ± 0.5 K. Then with this T_c, removing a Debye-Waller factor, using a linear term, and fixing $B_+ = B_-$ (duality) and $\alpha' = \alpha$ (scaling), they find $\alpha = 0.60 \pm 0.04$. The error bars are determined from variances resulting from changing T_c by ±1 K and excluding a window around T_c of 0 to 0.01 T_c. If either of the two equalities are not forced, the results are not changed significantly. The upper cutoff was set at $|t| = 0.03$, when the spot width became comparable to the cup aperture. (Note that this criterion is not sure to apply in all cases; other length scales associated with corrections to scaling may introduce nonlinearities to the log-log plot for smaller $|t|$.) As in our simulations, α_{eff} is below the pure value, but here less so, perhaps due to the smaller t's in the fitting range. Proceeding to the diffraction limit, Piercy and Pfnür use a small Faraday cup to measure the peak intensity below T_c (determined above). The log-log plot vs t is linear from 0.002 to 0.2; surprisingly, no nonlinear term is needed and the slope gives $2\beta = 0.17^{+0.03}_{-0.001}$, in excellent agreement with the pure value 1/6. Above T_c, they fit to a delta function plus Lorentzian, convoluting with a low T_c profile to represent the instrument response function. From log-log plots of χ and ξ vs t, they determine $\gamma = 1.08 \pm 0.07$ and $\nu = 0.68 \pm 0.03$ (compared with pure values of 7/6 and 2/3). The data are linear out to near 0.1, the largest t plotted. Finite-size rounding sets in around $t = -0.004$, corroborated by the non-vanishing of the delta-function component for $t < 0.004$.

At $\theta = 1/2$, preliminary measurements are made of a (2x2) phase composed of three rotationally related domains of p(2x1). This model is expected to be the universality class of the Heisenberg model with a face-centered anisotropy, known to have a first-order transition [11.77]. Nonetheless, they find Ising-like exponents: $\alpha = 0.01 \pm 0.02$ and $\beta = 0.13 \pm 0.02$. While one might be able to reinterpret the integrated intensity to mean $\alpha \simeq 1$, consistent with first-order critical scattering, the large value of β is mysterious.

11.3.2 Ising Systems

Even the search for a good Ising system has taken longer than was expected at ISISS-1981. An obvious category to study are overlayers with c(2x2) order on square lattices. The first attempt at Maryland, O/Ni{100} [11.78], proved unsatisfactory since upon disordering, the adatoms dissolve into the substrate, introducing uncontrollable bulk degrees of freedom. The next study was Cl/Ag{100} [11.79]. As the c(2x2) is heated to disordering, chlorine desorbs irreversibly, presumably due to very strong nearest neighbor repulsion. In this case, however, one can observe a reversible transition to the ordered state by increasing θ at fixed T. (For O/Ni{100}, there is a coexistence regime with p(2x2) on the low-coverage side of the pure c(2x2) phase.) To extract β, $\ell nI/\theta^2$ was plotted vs $\ell n(\theta-\theta_c)/(1/2-\theta_c)$, where θ_c is the coverage at the transition. The θ^{-2} was included to isolate the critical variation from the non-singular dependence on density, while the normalization of the coverage was chosen so that the fully ordered state at θ = 1/2 corresponds to T = 0. In this case one expects that (in the diffraction limit) $I \simeq (\mu-\mu_c)^{2\beta}$ as $\mu \rightarrow \mu_c^+$, where μ_c is the (unknown) chemical potential at the transition. Near the transition

$$\theta - \theta_c \simeq (\mu-\mu_c)^{1-\alpha} + \text{const}\cdot(\mu-\mu_c) \qquad (11.15)$$

so that (for $\alpha > 0$)

$$I \simeq (\theta-\theta_c)^{2\beta/(1-\alpha)}. \qquad (11.16)$$

Equation (11.16) is just an example of Fisher renormalization. By maximizing the linearity of the log-log plot, Taylor et al. estimated $\beta/(1-\alpha)$ = 0.12 ± 0.03; the value of θ_c, with error bars < 2%, was consistent with the point of inflection of I vs θ. The exponent is consistent with the Ising values of β = 1/8 and α = 0. However, this experiment was hardly ideal in that data in the disordered region were not adequate to permit corroborating extractions of γ and ν, and since less than a decade of abscissa scale was available. It is noteworthy that no nonlinearity appeared.

Another possible realization of the Ising model is a p(2x1) on a rectangular lattice. *Wang* and *Lu* studied O/W{112} as an example [11.80]. They analyze data over the range $0.002 \lesssim |t| \lesssim 0.11$ and quote exponents β = 0.13 ± 0.01, γ = 1.79 ± 0.14, and ν = 1.09 ± 0.11. Following a procedure popularized for physisorption [11.81], they do not use a log-log plot nor exclude the nonlinear, finite-size contaminated data near T_c. Instead, they take note of the fact that in addition to "smearing" the transition, finite size shifts the effective T_c. Since a real system contains a distribution of sizes of defect free regions, one convolutes the fitting function, e.g., $|t|^{2\beta}$, with a Gaussian distribution of T_c's. This procedure, for which no explicit justification has been published, implicitly parameterizes an unknown correction to scaling: It assumes that the shift in T_c is more important than the smearing of the transition. It assumes that corrections to scaling will be smaller if the reduced temperature is defined with respect to T_c of the finite-size system rather than the infinite system. The instrument response function is completely neglected, a reasonable approximation for synchrotron radiation ($L_i \sim 10^4$ Å), but not for LEED. In our opinion, it is not the best method; if used it should be checked with the procedures presented in Sect.11.3.

Two recent measurements of Ising behavior have captured theorists' attention [11.82]. *Kim* and *Chan* [11.83] studied the physisorption system CH_4/graphite foam with a.c. calorimetry. Evidence for Ising-like behavior include 1) logarithmic divergence of the specific heat, 2) a critical amplitude ratio (of the specific heat and so of energy-like anomalies) of unity, and 3) behavior of the phase boundary near its maximum (the width of the coexistence region going as $(-t)^{\beta}$).

In the other case, *Campuzano* et al. [11.84] studied the (1x2) reconstruction of the rectangular Au{110} surface. The experimenters used a novel mirror electron microscopy (MEMLEED) system [11.85], which promises ultrahigh resolution with instrument widths approaching 10^4 Å, although in this research more conventional resolution two orders of magnitude smaller was used. The reconstruction-induced spot was fit to a Gaussian plus a Lorentzian. Above T_c, from log-log plots over $0.04 \lesssim t \lesssim 0.2$ they quote γ = 1.75 ± 0.03 and ν = 1.02 ± 0.02. Below T_c, a log-log plot of the intensity of the Gaussian vs t, for $0.006 \lesssim |t| \lesssim 0.1$, is remarkably straight; the estimate of β is 0.13 ± 0.022. The quoted exponents are in excellent agreement with pure Ising values, but we believe the error bars of the critical-scattering exponents are rather optimistic, with ± 10% or so more in keeping with our model calculations and with other cited experiments. For example, we did a log-log fit of the exact Ising correlation length over the same thermal range and found T_c 0.5% too high and ν_{eff} = 0.89. Extracting data points from the published figures and trying some alterations of the fit, we produced similar values of ν_{eff}. A subsequent integrated-intensity measurement [11.86] of a reportedly better gold surface had a T_c 8% higher; in a fit over $0.004 \lesssim |t| \lesssim 0.035$ using (11.13) without the linear term (A_1 = 0) gave α = 0.02 ± 0.05. Given the low upper bound of the range, it is conceivable that the data were in the finite-size rounded regime, where analytic behavior is expected, and so might not be indicative of the critical behavior. Very recent work has also shown that trace Sn impurities can cause sizable shifts in T_c [11.87]. Possible explanations for the discrepant T_c's are recounted in [11.88].

An intriguing situation in which an Ising transition might occur is H/Ni(111) [11.89]. There H sits in both kinds of 3-fold sites with

comparable probability [11.89,90], indicative of a small or negligible binding energy difference. On this honeycomb lattice, with nearest neighbor exclusions due to the short spacing, one expects both types of sites to be occupied equally at low θ (and high T). As θ is increased, we expect an Ising transition to a phase in which either one of the kinds of sites is preferentially occupied [11.91,92]. Since the ordered state is p(1x1), there are no new diffraction features. However, with ion channeling one can distinguish occupancy in the two kinds of sites [11.90,93]. Unfortunately, in a realistically large sample one would expect domains of both varieties. Since this experiment measures the equivalent of the magnetization rather than its magnitude, much cancellation will occur, making detection difficult. As an aside, we note that the well-known graphitic (2x2) phase on this honeycomb net [11.89] is predicted to disorder in the 4-state Potts class [11.15,91]. An unfortunate but presumably surmountable barrier to such a study with LEED is the weak scattering of electrons by H.

11.3.3 XY with Cubic Anisotropy

We have not spent much time on the XY with cubic anisotropy universality class. Since the exponents are non-universal, this class is not optimal for comparison with theory. But the model has a rich range of behavior that will prove fascinating once there are a few more studies at the level of the Munich group's investigation of O/Ru{0001} to demonstrate feasibility. The prototype of this model is a net of spins, with nearest-neighbor dot-product interaction which can point in any direction in a plane but with an anisotropy field favoring alignment along any of four mutually perpendicular directions (e.g., N, E, S, W or NE, SE, SW, NW) [11.94]. In the limit of infinitely strong field, the spin can only point along these four directions, and the model reduces to Ising behavior. In the other limit of vanishing anisotropy the model reduces to the Kosterlitz-Thouless model, mentioned above in conjuction with the transition between floating and (incommensurate) disordered phases. At this unusual transition, $\ln \xi \propto |T - T_{KT}|^{-1/2}$ (rather than $-\nu \ln|t|$) and $\beta = \infty$; we also note that there is no anomaly in the specific heat at the transition [11.95].

Two transitions in this class have been studied. The work of *Lyuksyutov* and *Fedorus* [11.96] on H/W{110} was mentioned in [11.3] in a "note added in proof". They looked only for the exponent β, using the convolution-with-Gaussian-smearing method mentioned above. They estimated T_c as that value which gave the most linear log-log plot of $0.05 < |t| < 0.20$. For saturation coverage $\theta = 1/2$, they quote $\beta = 0.13 \pm 0.04$ based on data over the range $-0.05 < -t < 0.20$. (Note that with this procedure they are including data above T_c!) They were particularly interested in the coverage dependence of T_c, and indicate

that similar values of β were found at $\theta = 0.44$ and 0.51. Above $\theta = 0.60$, there is a (2x2) phase. At the saturation coverage $\theta = 0.75$, they estimate $\beta = 0.25 \pm 0.07$ with similar values at $\theta = 0.58$, 0.70, and 0.80. Given the rather inadequate nature of this early experiment, one must be cautious about placing too much weight on these numbers. Nonetheless, it is noteworthy that there is no indication of Fisher renormalization. This absence is consistent with the expected non-positive α for this model [11.97]. Then, in (11.15), the second, analytic term dominates near T_c and no renormalization occurs.

For W{100}, *Wendelken* and *Wang* [11.98] again followed the Russians' procedure. As in that study, only the long-range-order exponent β was measured. Wendelken and Wang simultaneously fit T_c, β, the amplitude of the assumed power law for the intensity, and the width of the Gaussian smearing function. The optimal set of values is quoted as 211 K, 0.144 ± 0.04, 1.76, and 3.26 K, respectively, for a flat surface. The primary goal of this brief report was to see how finite-size effects in the form of steps alter critical behavior. The domains on a flat surface are estimated to be of diameter 129 ± 20 Å, while on a stepped surface with terraces 30 Å wide; the lateral length of the domains is estimated as ~ 60 Å. For this stepped surface, the "best-fit" estimate of the four parameters is 217 K, 0.050 ± 0.01, 0.95, and 2.32 K, respectively. The strong dependence of β on T_c was noted, and the error bars on β were obtained by assuming $\pm$ 5 K error in T_c, with the comment that systematic errors should be in the same direction in both cases. In the flat case, pure power law behavior is observed only over the small range $0.03 < |t| < 0.08$; it would have been interesting to see how inclusion of a nonlinear term in the fitting form would have affected the results. It is not clear, however, that the data were robust enough to support an extra fitting parameter.

Another chemisoption system with a disordering transition in this class is the p(2x1)/W{110}. This system has been scrutinized by Lagally's group for nearly a decade [11.48]. Not only have equilibrium properties such as the phase diagram been thoroughly explored [11.99], even the kinetics of ordering have been investigated [11.100]. This system thus seems an excellent candidate unless it turns out that adsorption occurs in quasithreefold sites [11.60].

11.3.4 Se/Ni{100}: Realization of the Ashkin-Teller Model?

Based on symmetry arguments *Bak* et al. [11.68] suggested that the system Se/Ni{100} might be the first known realization of the Ashkin-Teller model [11.101]. Even though exponents have not yet been measured for this adsorption system, we include it here as an example of the exciting directions work in this field can take. The Ashkin-Teller model, which has been studied for over a quarter century for its in-

trinsic interest, consists of two distinct sets of Ising spins on a square lattice of sites, coupled by a quartic term. There are three phases: 1) at high T both Ising subsystems are disordered; 2) at low T both Ising subsystems are (ferromagnetically) ordered; 3) when the quartic interaction parameter is larger than the Ising coupling parameter and when T is moderately high, there is a remarkable "polarized" phase in which each Ising subsystem is disordered but the product of spins of the two subsystems (at the same site) has a non-zero expectation value. In the Ashkin-Teller model, the transition between this polarized phase and either of the other phases, which bound it, is in the Ising universality class while the transition between the ordered and disordered phases at small quartic coupling) is in the XY with cubic anisotropy class. The point at which the three phase boundaries intersect is in the 4-state Potts class. In Se/Ni{100}, the three phases are disordered, p(2x2), and c(2x2). One then makes the connection that the intensities of the (1/2, 0) and (0, 1/2) spots correspond, respectively, to the squared expectation value of each the two Ising subsystems, while the (1/2, 1/2) beam corresponds to the squared "polarization". Thus, the transition between the c(2x2) and either p(2x2) or disordered [(1x1)] is expected to be Ising-like while that between p(2x2) and disorder should be like XY with cubic anisotropy, consistent with Landau assignments (cf. Table 11.1). In addition, the multicritical point where the three lines meet, i.e., where the upper boundary of the c(2x2) phase drops to meet the top of the p(2x2) phase, should have 4-state Potts symmetry. The competition between the critical behavior associated with the different transitions leads to crossover effects (discussed generically in [11.3]), impeding extraction of exponents either in a numerical study (e.g. our transfer matrix scaling work) or in a diffraction measurement. Testing these predictions poses a formidable but intriguing challenge.

11.4 Conclusions

In assessing the current status of the field, we see that a few good systems have been well studied. It will be gratifying to find realizations of the various universality classes. The thermal range that is probed in present experiments is on the order of a single decade (an improvement over the half decade used for O/Ni{111} [11.4,41]), going from reduced temperatures of order 10^{-2} to 10^{-1}. This range pales in comparison with 3D fluids (which, however, have much smaller critical fluctuations): ranges of $3 \cdot 10^{-6}$ - 10^{-4} for binary fluids [11.102] and 10^{-6} - 10^{-2} for liquid helium [11.103] have been attained. On the other hand, it is far superior to spin glasses [11.104], where the nonlinear susceptibility is measured over the range 0.15 - 0.3. The importance of large defect-free regions, to allow small $|t|_{min}$, should be obvious.

While the pure exponents of the various classes are firmly established, theoretical questions remain about which corrections to scaling are present in particular systems [11.23]. In order to contribute to this intriguing research, experiments will need to be improved by an order of magnitude, if not more. It now appears that in some cases, e.g., Pt{111} [11.49,105], defect-free regions as large as 1000-2000 Å have been achieved. (If better metallic surfaces cannot be obtained in other cases, attempts should be made to grow on high-grade graphite, mica, or MgO, although in most cases the metal will bead up; see for example [11.106].) This will allow the closer approach to T_c needed to investigate intriguing corrections to scaling. To take advantage of better surfaces, higher resolution will be needed. Several labs now have high-resolution LEED systems. MEMLEED promises even better resolution [11.85]. X-ray radiation from synchrotrons has already demonstrated it [11.107], but now must attain the sensitivity needed for measurements of submonolayers. Note that in this desired scenario, the critical scattering will be a much smaller fraction of the long-range order, heightening the need for improved sensitivity. In contrast with the integrated intensity approach, any surface science laboratory can look at critical properties in the course of characterizing a sample with a phase transition. But, as we have emphasized, it is important to have several exponents. Measurements below T_c, i.e., in the ordered state are more prone to systematic errors than those above; experimentalists should not just content themselves with extraction of the most obvious exponent, β.

At the same time, more systems should be studied with current methods so that as improved apparatus and sample preparation are possible, it will be clear where to apply them. Several possibilities have been mentioned in the text. *Unertl* [11.14] mentions as examples of systems ripe for measurement the following: Se/Ni{001}, S/Ni{111}, Te/Ni{111}, Bi/Cu{111}, H/W{001}, [H/]Mo{001}, and S/Mo{110}. It would be particularly interesting to find a good 3-state Potts transition; the disordering of ($\sqrt{3}$x$\sqrt{3}$) phases of I/Cu{111} [11.108] and S/Pt{111} [11.109] deserve further attention.

Two topics reviewed here in 1983 are especially suitable for investigation in chemisorption systems. Vigorous study of incommensuration [11.11] is worthwhile. This problem is being actively pursued in physisorption systems [11.107] and in crystal growth [11.50]. In the chemisorption literature, there are many reports of streaking or splitting of sharp spots as coverage is increased beyond the saturation value of an ordered monlayer, as well as of a region labeled "antiphase domains". It is important but difficult to distinguish between floating phases and incommensurate disordered phases. In "strong" chemisorption, the adatoms will always be in registry, so that domain walls will be sharp.

The systematics of finite-size [11.110] effects also deserve close attention. Once a high-quality surface has been attained and measured, L_s can be systematically reduced with the addition of point defects, either by the adsorption of very strongly bound "impurity" atoms [11.111] or by the creation of local defects using sputtering. Alternatively, as applied by *Wendelken* and *Wang* [11.98], one can consider vicinal surfaces, leading to asymmetric reduction in L_s.

The most exciting recent development in the theory of 2D phase transitions is the application of ideas from conformal invariance [11.112]. At T_c, when ξ is infinite, correlation functions are conformally covariant. (This local property is considerably more restrictive than the [global] covariance under scale change that underlies renormalization group procedures.) In 2D, this fact is particularly useful since all analytic functions are conformal transformations. The analysis only applies to systems with isotropic interactions (e.g., not to (3x1)/centered rectangular). This rather esoteric line of study has led to an explanation of why the critical exponents (including correction-to-scaling exponents [11.23]) are rather simple rational fractions. For purposes of comparison with experiment, one should consider the lineshape $S(k,T_c)$, (in principle also) including the effects of multiple scattering. *Kleban* et al. [11.88,113,114] have poineered this challenging research, presenting results for the Ising model, with explicit calculations in the simplifying approximation of s-wave scattering. Recall that the data around T_c were excluded from earlier scaling analyses as being contaminated by finite-size effects. Near T_c, one finds the scaling form [11.113,115]

$$S(k,T,L_s) \sim L_s^{4-\eta}\, X_{\pm}(k\xi,kL_s) \rightarrow L_s^{4-\eta}\, Y(kL_s) \quad [T=T_c] \qquad (11.17)$$

where Y depends explicitly on the shape and boundary conditions of the scattering lattice and $\eta = 2 - \gamma/\nu \rightarrow 1/4$ for the Ising model. Since conformal invariance is a continuum theory, the simple form of (11.17) must break down when k gets so large that the lattice constant becomes significant; explicit tests [11.115] show that (11.17) holds for k less than about 1/4 of a reciprocal lattice spacing. Moreover, for geometries that are not very anisotropic, the shape dependence is relatively weak, so that one can approximate the domain as circular [11.88]. (In the limit of large anisotropy of the domain, such as vicinal surfaces, there may be notable anisotropic effects.) To a good approximation, the lineshape can be represented by a Gaussian plus a Lorentzian, with the ratio of their heights and their widths explicitly given. These predictions have been tested, with good agreement, on experimental data for the (1x2) reconstruction of Au{110} [11.88]. (The asymmetry of the microscopic interactions in the rectangular Au{110}

can be trivially rescaled to attain an isotropic situation [11.116].) With the advent of better surfaces, more detailed tests should be possible.

With these new developments and possibilities mentioned earlier in this section, one would expect this exciting area to be booming; unfortunately, this is not the case. I offer some personal comments on the situation. The field is a demanding one for surface scientists in terms of both the background theory and the actual experiments. The rewards in terms of practical applications are less immediately apparent than in other pursuits in surface science. Much of the problem, however, is "sociological". The major seminal breakthroughs in theory came about a decade ago. Experiments were slow to follow, and many of the leading theorists moved on to other topics. Now that reasonable experiments are becoming feasible, the field is viewed by enough peer reviewers as passé to threaten funding in these competitive, trendy times. I find it tragic and perverse that the field is languishing while on the verge of great progress.

Acknowledgements. Most of our reseearch has been supported by the Department of Energy under grant DE-FG05-84ER45071. Computer facilities were supplied by the University of Maryland Computer Science Center. Partial funding presently was obtained from NSF grant DMR-85-04163 and NATO grant 86/0782. I also acknowledge the hospitality, as a guest worker of the Surface Science Division of the National Bureau of Standards, Gaithersburg, MD. The research described herein was done in extended collaboration with N.C. Bartelt and L.D. Roelofs, without whose energy and insight it would have been impossible. I thank the former also for helpful comments on the manuscript. Ongoing fruitful interactions with E.D. Williams and R.L. Park and their many talented students have been crucial to our program. Many colleagues elsewhere have contributed preprints and helpful conversations; at the risk of offending the omitted, I mention P.H. Kleban, W.N. Unertl, H. Pfnür, J.C. Campuzano, A.L. Stella, U. Glaus, S. Fishman, J.G. Amar.

References

11.1 For a review of reconstruction, see P.J. Estrup: In *Chemistry and Physics of Solid Surfaces V*, ed. by R. Vanselow, R. Howe (Springer, Berlin, Heidelberg 1984) p.205

11.2 For a review, see K. Binder: In *Phase Transitions and Critical Phenomena*, ed by C. Domb, J.L. Lebowitz, Vol.8 (Academic, London 1983), p.1

11.3 T.L. Einstein: In *Chemistry and Physics of Solid Surfaces IV*, ed. by R. Vanselow, R. Howe (Springer, Berlin, Heidelberg 1982) p.251

11.4 L.D. Roelofs, A.R. Kortan, T.L. Einstein, R.L. Park: Phys. Rev. Lett. 46, 1465 (1981)

11.5 N.C. Bartelt, T.L. Einstein, L.D. Roelofs: J. Vac. Sci. Tech. A 1, 1217 (1983)

11.6 N.C. Bartelt, T.L. Einstein, L.D. Roelofs: Phys. Rev. B 35, 1776 (1987)

11.7 N.C. Bartelt, T.L. Einstein, L.D. Roelofs: Phys. Rev. B 32, 2993 (1985)

11.8 N.C. Bartelt, T.L. Einstein, L.D. Roelofs: Phys. Rev. B 35, 4812 (1987)

11.9 N.C. Bartelt, T.L. Einstein, L.D. Roelofs: Phys. Rev. B 35, 6786 (1987)

11.10 An excellent general reference on critical phenomena is a) P. Pfeuty, G. Toulouse: *Introduction to the Renormalization Group and Critical Phenomena* (Wiley, New York 1977);
see also b) M.E. Fisher: In *Collective Properties of Physical Systems*, ed. by

B. Lundqvist, S. Lundqvist (Proc. 24th Nobel Symposium, Academic, New York 1973) p.16;
c) S.-K. Ma: *Modern Theory of Critical Phenomena* (Benjamin, Reading, Mass. 1976)
11.11 P. Bak: In *Chemistry and Physics of Solid Surfaces V*, ed. by R. Vanselow, R. Howe (Springer, Berlin, Heidelberg 1984) p.317
11.12 L. Passell, S.K. Satija, M. Sutton, J. Suzanne: In *Chemistry and Physics of Solid Surfaces VI*, ed. by R. Vanselow, R. Howe (Springer, Berlin, Heidelberg 1986) p.609
11.13 T.L. Einstein: In Proc. 10th Johns Hopkins Workshop. *Infinite Lie Algebras and Conformal Invariance in Condensed Matter and Particle Physics*, ed. by K. Dietz, V. Rittenberg (World Scientific, Singapore 1987) p.17
11.14 W.N. Unertl: Comments Cond. Mat. Phys. 12, 289 (1986)
11.15 M. Schick: Prog. Surf. Sci. 11, 245 (1981);
see also E. Domany, M. Schick, J.S. Walker, R.B. Griffiths: Phys. Rev. B 18, 2209 (1978);
S. Alexander: Phys. Lett. 54A, 353 (1075)
11.16 For a review of Potts models see F.Y. Wu: Rev. Mod. Phys. 54, 235 (1982)
11.17 D.A. Huse, M.E. Fisher: Phys. Rev. Lett. 49, 793 (1982); Phys. Rev. B 29, 239 (1984)
11.18 M.P.M. den Nijs: J. Phys. A 17, L295 (1984)
11.19 P.A. Bennett, M.B. Webb: Surf. Sci. 104, 74 (1981);
E.G. McRae, R.A. Malic: Surf. Sci. 148, 551 (1984)
11.20 M. Trenary, K.J. Uram, F. Bozso, J.T. Yates, Jr.: Surf. Sci. 146, 269 (1984)
11.21 R.J. Phaneuf, M.B. Webb: Surf. Sci. 164, 167 (1985)
11.22 A. Aharony, M.E. Fisher: Phys. Rev. B 27, 4394 (1983)
11.23 H.W.J. Blöte, M.J.M. den Nijs: Phys. Rev. B 37, 1766 (1987)
11.24 N.C. Bartelt, T.L. Einstein, L.D. Roelofs: Phys. Rev. Lett. 56, 2881 (1986)
11.25 S. Dietrich, H. Wagner: Phys. Rev. Lett. 51, 1469 (1983);
see also W. Moritz, M.G. Lagally: Phys. Rev. Lett. 56, 865 (1986)
11.26 M. Fink, J. Ingram: At. Data 4, 1 (1972);
M.B. Webb, M.G. Lagally: Solid State Phys. 28, 301 (1973)
11.27 M.E. Fisher: Phys. Rev. 176, 257 (1968)
11.28 R.L. Park, J.E. Houston, D.G. Schreiner: Rev. Sci. Instrum. 42, 60 (1971)
11.29 M. Henzler: Surf. Sci. 152/153, 963 (1985);
M.G. Lagally: Appl. Surf. Sci. 13, 260 (1982);
M.G. Lagally, J.A. Martin: Rev. Sci. Instrum. 54, 1273 (1983);
U. Scheithauer, G. Meyer, M. Henzler: Surf. Sci. 178, 441 (1986)
11.30 T. Engel: In *Chemistry and Physics of Solid Surfaces V*, ed. by R. Vanselow, R. Howe (Springer, Berlin, Heidelberg 1984) p.257, and this volume
J.P. Toennies: private commun.
11.31 M. Schick: Phys. Rev. Lett. 51, 1347 (1981)
11.32 J.F. Nicoll, J.K. Bhatarcharjee: Phys. Rev. B 23, 389 (1981);
J.F. Nicoll, P.C. Albright: ibid. 31, 4576 (1985)
11.33 K. Binder: J. Stat. Phys. 24, 69 (1981);
K. Binder, D.P. Landau: Phys. Rev. Lett. 52, 318 (1984);
see also M. Fähnle, J. Souletie: J. Phys. C 17, L469 (1984); Phys. Rev. B 32, 3328 (1985);
A.S. Arrott: ibid. 31, 2851 (1985)
11.34 J.V. Sengers: private commun.
11.35 B. Nienhuis: J. Phys. A 15, 199 (1982)
11.36 J.L. Cardy, M. Nauenberg, D.J. Scalapino: Phys. Rev. B 22, 2560 (1980)
11.37 C.A. Tracy, B.M. McCoy: Phys. Rev. B 12, 368 (1975);
E. Barouch, B.M. McCoy, T.T. Wu: Phys. Rev. Lett. 31, 1409 (1973)

11.38 M.E. Fisher, J.S. Langer: Phys. Rev. Lett. 20, 665 (1978);
see also M. Ferer, M.A. Moore, M. Wortis: ibid. 22, 1382 (1969)
11.39 A.D. Bruce: J. Phys. C 7, 2089 (1974)
11.40 N.C. Bartelt, T.L. Einstein, L.D. Roelofs: J. Vac. Sci. Tech. A 3, 1568 (1985)
11.41 N.C. Bartelt, T.L. Einstein, L.D. Roelofs: In *The Structure of Surfaces*, ed. by M.A. van Hove, S.Y. Tong (Springer, Berlin, Heidelberg 1985) p.357
11.42 J. Henrion, G.E. Rhead: Surf. Sci. 29, 20 (1972)
11.43 M. Kaufmann, D. Andelman: Phys. Rev. B 29, 4010 (1984)
11.44 K.D. Miner, M.H.W. Chan, A.D. Migone: Phys. Rev. Lett. 51, 1465 (1983)
11.45 J.H. Campbell, M. Bretz: Phys. Rev. B. 32, 2861 (1985)
11.46 Y. Saito: Phys. Rev. B 24, 6652 (1981);
K. Binder: J. Stat. Phys. 24, 69 (1981);
W. Selke, J. Yeomans: Z. Phys. B 46, 311 (1982)
11.47 An exception is K.K. Chan, M. Deutsch, B.M. Ocko, P.S. Pershan, L.B. Sorensen: Phys. Rev. Lett. 54, 920 (1985)
11.48 M.G. Lagally, G.-C. Wang, T.-M. Lu: In *Chemistry and Physics of Solid Surfaces II*, ed. by R. Vanselow (CRC, Boca Raton 1979) p.153
11.49 K. Kern, P. Zeppenfeld, R. David, G. Comsa: In *The Structure of Surfaces-II*, ed. by J.F. van der Veen, M.A. Van Hove (Springer, Berlin, Heidelberg 1988)
11.50 J.H. van der Merwe: *Chemistry and Physics of Solid Surfaces V* ed. by R. Vanselow, R. Howe (Springer, Berlin, Heidelberg 1984) p.365;
J.M. Moison, C. Guille, M. Bensoussan: In *The Structure of Surfaces-II*, ed. by J.F. van der Veen, M.A. van Hove (Springer, Berlin, Heidelberg 1988)
11.51 P. Dutta, S.K. Sinha: Phys. Rev. Lett. 47, 50 (1981)
11.52 D.A. Huse: J. Phys. A 16, 4357 (1983)
11.53 R.J. Baxter: J. Phys. A 13, L61 (1980); *Exactly Solved Models in Statistical Mechanics* (Academic, London 1982);
R.J. Baxter, P.A. Pearce: J. Phys. A 15, 897 (1982)
11.54 A.L. Stella, X.-C. Xie, T.L. Einstein, N.C. Bartelt: Z. Phys. B 67, 357 (1987), and references therein
11.55 M.E. Fisher: J. Stat. Phys. 34, 667 (1984)
11.56 S.N. Coppersmith, D.S. Fisher, B.I. Halperin, P.A. Lee, W.F. Brinkman: Phys. Rev. B 25, 349 (1982)
11.57 D. Nelson: In *Phase Transitions and Critical Phenomena*, Vol.7, ed. by C. Domb, J.L. Lebowitz (Academic, New York 1983)
11.58 R. Imbihl, R.J. Behm, K. Christman, G. Ertl, T. Matsushima: Surf. Sci. 117, 257 (1982)
11.59 W. Kinzel, W. Selke, K. Binder: Surf. Sci. 121, 13 (1982)
11.60 W. Moritz, R. Imbihl, R.J. Behm, G. Ertl, T. Matsushima: J. Chem. Phys. 83, 1959 (1985)
11.61 L.D. Roelofs: In *Chemistry and Physics of Solid Surfaces IV*, ed. by R. Vanselow, R. Howe (Springer, Berlin, Heidelberg 1982), p.219
11.62 A.R. Kortan, R.L. Park: Phys. Rev. B 23, 6340 (1981)
11.63 K. Binder, D.P. Landau: Phys. Rev. B 30, 1477 (1984);
M.S.S. Challa, D.P. Landau, K. Binder: Phys. Rev. B 34, 1841 (1986);
K. Binder, D. Stauffer: In *Application of the Monte Carlo Method in Statistical Physics*, ed. by K. Binder (Springer, Berlin, Heidelberg 1984) Chap.1;
K. Binder: Rep. Prog. Phys. 50, 783 (1987), Ref.18.a
11.64 K. Binder: J. Stat. Phys. 24, 69 (1981)
11.65 M.E. Fisher, A.N. Berker: Phys. Rev. B 26, 2507 (1982)
11.66 M. Schick: Phys. Rev. Lett. 47, 1347 (1981)
11.67 G. Grest, M. Widom: Phys. Rev. B 24, 6508 (1981)
11.68 P. Bak, P.H. Kleban, W.N. Unertl, J. Ochab, G. Akinci, N.C. Bartelt, T.L. Einstein: Phys. Rev. Lett. 54, 1539 (1985)

11.69 I.G. Enting: J. Phys. A 8, 1681 (1975)
11.70 W. Witt, E. Bauer: Ber. Bunsenges. Phys. Chem. 90, 248 (1986)
11.71 A recent review is: G. Grinstein: In *Fundamental Problems in Statistical Mechanics*, ed. by E.G.D. Cohen (Elsevier, Amsterdam 1985) Vol.6, p.147
11.72 W. Kinzel: Phys. Rev. B 27, 5819 (1983);
L.D. Roelofs: Appl. Surf. Sci. 11/12, 425 (1982);
R. Birgeneau, A.N. Berker: Phys. Rev. B. 26, 3751 (1982)
11.73 H. Ohtani, C.-T. Kao, M.A. Van Hove, G.A. Somorjai: Prog. Surf. Sci. 23, 155 (1987);
G.A. Somorjai: *Chemistry in Two Dimensions: Surfaces* (Cornell U. Press, Ithaca 1981);
G.A. Somorjai, F.Z. Szalkowski: J. Chem. Phys. 54, 389 (1971)
11.74 Peder Estrup remarked to me recently, "There are no simple chemisorption systems!"
11.75 R.Q. Hwang; E.D. Williams, R.L. Park: Surf. Sci. Lett. 193, L53 (1988)
11.76 P. Piercy, H. Pfnür: Phys. Rev. Lett. 59, 1124 (1987);
P. Piercy, M. Maier, H. Pfnür: In *The Structure of Surfaces-II* , ed. by J.F. van der Veen, M.A. Van Hove (Springer, Berlin, Heidelberg 1988)
11.77 B. Nienhuis, E.K. Riedel,M. Schick: Phys. Rev. B 27, 5625 (1983);
M.Schick: Surf. Sci. 125, 94 (1983)
11.78 D.E. Taylor, R.L. Park: Surf. Sci. 125, L73 (1983)
11.79 D.E. Taylor, E.D. Williams, R.L. Park, N.C. Bartelt, T.L. Einstein: Phys. Rev. B 32, 4653 (1985)
11.80 G.-C. Wang, T.-M. Lu: Phys. Rev. B 31, 5918 (1985)
11.81 P.M. Horn, R.J. Birgeneau, P. Heiney, E.M. Hammonds: Phys. Rev. Lett. 41, 961 (1978)
11.82 M.E. Fisher: J. Chem. Soc., Faraday Trans. II 82, 1569 (1986)
11.83 H.K. Kim, M.H.W. Chan: Phys. Rev. Lett. 53, 170 (1984)
11.84 J.C. Campuzano, M.S. Foster, G. Jennings, R.F. Willis, W.N. Unertl: Phys. Rev. Lett. 54, 2684 (1985);
J.C. Campuzano, G. Jennings, R.F. Willis: Surf. Sci. 162, 484 (1985)
11.85 M.S. Foster, J.C. Campuzano, R.F. Willis, J.C. Dupuy: J. Microscopy 140, 395 (1985)
11.86 D.E. Clark, W.N. Unertl, P.H. Kleban: Phys. Rev. B 34, 4379 (1986)
11.87 E.G. McRae, T.M. Buck, R.A. Malic, G.H. Wheatley: Phys. Rev. B 36, 2341 (1987)
11.88 P.H. Kleban, R. Hentschke, J.C. Campuzano: Phys. Rev. B 37, 5788 (1988)
11.89 K. Christmann, R.J. Behm, G. Ertl, M.A. Van Hove, W.H. Weinberg: J. Chem. Phys. 70, 4168 (1979)
11.90 F. Besenbacher, I. Stensgaard, K. Mortensen: In *The Structure of Surfaces-II*, ed. by J.F. van der Veen, M A. Van Hove (Springer, Berlin, Heidelberg 1988);
F. Besenbacher: private commun.
11.91 L.D. Roelofs, T.L. Einstein, N.C. Bartelt, J.D. Shore: Surf. Sci. 176, 295 (1986)
11.92 W.M. Gibson: In *Chemistry and Physics of Solid Surfaces V*, ed. by R. Vanselow, R. Howe (Springer, Berlin, Heidelberg 1984) p.427;
T. Gustafsson: In *The Structure of Surfaces-II*, ed. by J.F. van der Veen, M.A. Von Hove (Springer, Berlin, Heidelberg 1988)
11.93 E. Domany, M. Schick: Phys. Rev. B 20, 3828 (1979)
11.94 J.V. José, S. Kirkpatrick, L.P. Kadanoff, D.R. Nelson: Phys. Rev. B 16, 1217 (1977)
11.95 J.M. Kosterlitz, D.J. Thouless: J. Phys. C 6, 1181 (1973); Ref.38
11.96 I.F. Lyuksyutov, A.G. Fedorus: Sov. Phys. JETP 53, 1317 (1981) [Zh. Eksp. Teor. Fiz. 80, 2511 (1981)]

11.97 G.-Y. Hu, S.-C. Ying: [Physica 140 A, 585 (1987)] argue that ν increases monotonically from 1 to ∞ along the line of transitions, implying by hyperscaling that α decreases from 0 to $-\infty$.
11.98 J.F. Wendelken, G.-C. Wang: Phys. Rev. B 32, 7542 (1985)
11.99 G.-C. Wang, M.G. Lagally: Surf. Sci. 81, 69 (1979);
M.G. Lagally, T.-M. Lu, G.-C. Wang: In *Ordering in Two Dimensions*, ed. by S.K. Sinha (North-Holland, New York, Amsterdam 1980) p.113
11.100 M.C. Tringides, P.K. Wu, M.G. Lagally: Phys. Rev. Lett. 59, 315 (1987)
11.101 J. Ashkin, E. Teller: Phys. Rev. 64, 178 (1943)
11.102 R.F. Chang, H. Burstyn, J.V. Sengers: Phys. Rev. B 19, 866 (1979)
11.103 G. Ahlers: Rev. Mod. Phys. 52, 489 (1980)
11.104 P. Mazumdar, S.M. Bhagat: J. Mag. & Mag. Mat. 66, 263 (1987)
11.105 G. Comsa: private commun.
11.106 L. Holland: *Vacuum Deposition of Thin Films* (Wiley, New York 1961)
11.107 R.J. Birgeneau, G.S. Brown, P.M. Horn, D.E. Moncton, P.W. Stephens: J. Phys. C 14, L49 (1981);
P.W. Stephens, P.A. Heiney, R.J. Birgeneau, P. Horn, D.E. Moncton, G.S. Brown: Phys. Rev. B 29, 3512 (1984)
11.108 S.B. DiCenzo, G.K. Wertheim, D.N.E. Buchanan: Surf. Sci. 121, 411 (1982)
11.109 M. Auer, H. Leonhard, K. Hayek: Appl. Surf. Sci. 17, 70 (1983)
11.110 P.H. Kleban: In *Chemistry and Physics of Solid Surfaces V*, ed. by R. Vanselow, R. Howe (Springer, Berlin, Heidelberg 1984) p.339;
M.N. Barber: In *Phase Transitions and Critical Phenomena*, Vol.8, ed. by C. Domb, J.L. Lebowitz (Academic, London 1984) p.145
11.111 D.W. Goodman: In *Chemistry and Physics of Solid Surfaces VI*, ed. by R. Vanselow, R. Howe (Springer, Berlin, Heidelberg 1986) p.169
11.112 For an excellent introductory review, see J.L. Cardy: In *Phase Transitions and Critical Phenomena*, Vol.11, ed. by C. Domb, J.L. Lebowitz (Academic, London 1986)
11.113 P.H. Kleban, G. Akinci, R. Hentschke, K.R. Brownstein: J. Phys. A 19, 437 (1986); Surf. Sci. 166, 159 (1986)
11.114 R. Hentschke, P.H. Kleban: Surf. Sci., to be published
11.115 N.C. Bartelt, T.L. Einstein: J. Phys. A 19, 1429 (1986)
11.116 M.P. Nightingale, H. Blöte: J. Phys. A 16, 1657 (1983)